Letter

Minimal model for the flat bands in copper-substituted lead phosphate apatite: Strong diamagnetism from multiorbital physics

Omid Tavakol and Thomas Scaffidi*

Department of Physics and Astronomy, University of California, Irvine, California 92697, USA

Department of Physics, University of Toronto, 60 St. George Street, Toronto, Ontario M5S 1A7, Canada

(Received 23 October 2023; revised 14 February 2024; accepted 23 February 2024; published 11 March 2024)

The claims that a copper-substituted lead apatite, denoted as $CuPb_9(PO_4)_6(OH)_2$, could be a room-temperature superconductor have led to intense research activity. While other research groups did not confirm these claims, and the hope of realizing superconductivity in this compound has all but vanished, other findings have emerged which motivate further work on this material. In fact, density functional theory calculations indicate the presence of two nearly flat bands near the Fermi level, which are known to host strongly correlated physics. To facilitate the theoretical study of the intriguing physics associated with these two flat bands, we propose a minimal tight-binding model which reproduces their main features. We then calculate the orbital magnetic susceptibility of our two-band model and find a large diamagnetic response which arises due to the multiorbital nature of the bands and which could provide an explanation for the strong diamagnetism reported in experiments.

DOI: 10.1103/PhysRevB.109.L100504

Introduction. Recently, copper-substituted lead apatite $CuPb_9(PO_4)_6(OH)_2$ was proposed as a room-temperature superconductor [1,2]. While superconductivity in this material was not replicated by other groups, a density functional theory (DFT) calculations recently predicted the appearance of two nearly flat bands in this material close to the Fermi level [3] (see also Refs. [4–9]). Since flat bands are known to host strongly correlated physics [10–13], this motivates additional research on $CuPb_9(PO_4)_6(OH)_2$. In addition, the reported unusual magnetic properties of this material—a combination of soft ferromagnetism and strong diamagnetism [14]—provide further motivation. To study the potentially rich physics hosted by the two flat bands, it would be beneficial to have a minimal two-band model which reproduces their main qualitative features. In this Letter, we propose such a minimal model, and discuss the implications for superconductivity and diamagnetism.

Following Ref. [3], we investigate the situation in which Pb is substituted by Cu on one of the four Pb(1) sites of the lead apatite structure. (Here we follow the nomenclature in Ref. [3] for which Pb(1) sites occupy the Wyckoff $4f$ positions of space group 176 $P6_3/m$ but we note that the name Pb(2) also appears for these sites in the literature.) Reference [3] predicts the existence close to the Fermi level of two isolated flat bands with a small bandwidth (around 0.1 eV), which are well-separated from all the other bands. Since these two bands are predicted to be mostly of Cu d_{zx} and d_{zy} character, we aim to write a minimal tight-binding two-orbital model. Even though they have a small bandwidth, these two bands still have a nonzero momentum dependence (see Fig. 4 of Ref. [3]) which should be important for the physics, and which we hope to reproduce with our model. If we neglect the small z shift of their $4f$ Wyckoff position, the four Pb(1) sites form two honeycomb layers stacked along z. We thus use a simplified structure for which the Cu sites occupy one sublattice (called A) of a honeycomb lattice, and are stacked vertically on every other layer (see Fig. 1).

Before moving on to the model, it is worth noting that a multitude of DFT results [3–9] concerning this compound have emerged with sometimes conflicting results. In particular, the question of whether LK-99 is a metal or a Mott insulator has received conflicting answers which depend sensitively on the size of the Hubbard U parameter and the relaxation of the structure. Although metallic behavior was reported in Ref. [3] on which our model is based, subsequent studies have reported the opening of a gap once the structure is fully relaxed [6]. Further work has also shown that the way in which correlations are treated is crucial, since Ref. [8] found the opening of a gap within quasiparticle self-consistent GW, regardless of the relaxation stage of the structure. In addition, Ref. [9] showed how the Perdew-Burke-Ernzerhof (PBE) functional predicts a metallic state with two flat bands close to the Fermi level in overall agreement with Ref. [3], whereas PBE+U shows a charge-transfer gap gradually opening as U is increased. In this context, our approach is to build a model which can reproduce the metallic band structure before the formation of a many-body band gap due to strong repulsion. The tight-binding model in Eq. (1) is thus only intended to serve as the kinetic energy contribution to a multiorbital Hubbard model which should also include a Hubbard-U term which would most likely open a many-body gap for relevant values of U. Since our analysis of superconductivity and magnetism assumes a metallic state, it might not be directly relevant to LK-99 if that compound is confirmed to be a charge-transfer or Mott insulator, but still holds value as a theoretical study of our two-orbital model in the small U regime.

*tscaffid@uci.edu

Model. We propose the following single-particle Hamiltonian $H_0 = \sum_{\mathbf{k}} c^\dagger_{\mathbf{k},a} H_{a,b}(\mathbf{k}) c_{\mathbf{k},b}$ with

$$H_{a,b}(\mathbf{k}) = d_v(\mathbf{k})\sigma^v_{a,b} - \mu\delta_{a,b}, \tag{1}$$

with $\sigma^v = (\mathbf{1}, \sigma^x, \sigma^y, \sigma^z)$ the Pauli matrices written in the orbital basis indexed by $a, b = \{d_{zx}, d_{zy}\}$, with μ the chemical potential and with

$$d_0(k) = -\frac{1}{2}\left(\frac{1}{2}\sum_{i=1,2,3}\cos(\mathbf{k}\cdot\mathbf{b}_i) + 3\right) - 2t_z\cos(k_z), \tag{2}$$

$$d_1(k) = -\frac{\sqrt{3}}{4}(-\cos(\mathbf{k}\cdot\mathbf{b}_1) + \cos(\mathbf{k}\cdot\mathbf{b}_2)),$$

$$d_2(k) = -\frac{\sqrt{3}}{4}(\sin(\mathbf{k}\cdot\mathbf{b}_3) + \sin(\mathbf{k}\cdot\mathbf{b}_2) + \sin(\mathbf{k}\cdot\mathbf{b}_1)),$$

$$d_3(k) = -\frac{1}{2}\left(\cos(\mathbf{k}\cdot\mathbf{b}_3) - \frac{1}{2}(\cos(\mathbf{k}\cdot\mathbf{b}_1) + \cos(\mathbf{k}\cdot\mathbf{b}_2))\right),$$

where we used the lattice vectors connecting nearest-neighbor Cu sites: $\mathbf{b}_1 = -\sqrt{3}/2\hat{e}_x + 3/2\hat{e}_y$, $\mathbf{b}_2 = -\sqrt{3}/2\hat{e}_x - 3/2\hat{e}_y$, and $\mathbf{b}_3 = \sqrt{3}\hat{e}_x$. In real space, this Hamiltonian reads

$$\begin{aligned} H_0 = &\sum_{\mathbf{r}}\left(-\mu - \frac{3}{2}\right)c^\dagger_{\mathbf{r},a}c_{\mathbf{r},a} \\ &- \sum_{\mathbf{r}}\sum_{i=1,2,3} c^\dagger_{\mathbf{r},a}(\mathcal{T}_i)_{a,b}c_{\mathbf{r}+\mathbf{b}_i,b} + \text{H.c.} \\ &- t_z\sum_{\mathbf{r}} c^\dagger_{\mathbf{r},a}c_{\mathbf{r}+c\hat{z},a} + \text{H.c.}, \end{aligned} \tag{3}$$

where $\mathbf{r}$ is summed over Cu sites, c is the lattice spacing between copper sites along the z axis, and the hopping matrices are given by

$$\mathcal{T}_1 = \begin{pmatrix} 0 & -\frac{\sqrt{3}}{4} \\ 0 & \frac{1}{4} \end{pmatrix}, \tag{4}$$

and

$$\mathcal{T}_2 = \begin{pmatrix} 0 & 0 \\ \frac{\sqrt{3}}{4} & \frac{1}{4} \end{pmatrix}, \tag{5}$$

and

$$\mathcal{T}_3 = \begin{pmatrix} \frac{3}{8} & -\frac{\sqrt{3}}{8} \\ \frac{\sqrt{3}}{8} & \frac{-1}{8} \end{pmatrix}. \tag{6}$$

The $-3/2$ potential term can of course be absorbed in the chemical potential but we keep it as it makes the connection to the honeycomb p_x, p_y honeycomb model more transparent [15], as we show below.

This Hamiltonian contains hopping terms to the 6 nearest-neighbors on the triangular lattice of the Copper sites (see arrows in Fig. 1), and to the two nearest-neighbors along the z axis [the Pb(1) sites are stacked on top of each other along the z axis]. We calculated the orbital-dependent hopping terms by starting from a four-band honeycomb lattice model [15] with a d_{zx} and d_{zy} orbital on every site, and for which only σ-bonding terms are included, which means there is a single hopping term for each bond which generates a coupling between the projection of orbitals on the bond direction. We then added a strong staggered potential ϵ which gaps out the B sublattice, leaving behind a two-band model for the A sublattice. (Such a staggered potential in the four-band model was studied in Ref. [16].) At leading order in perturbation theory in $1/\epsilon$, we obtain the tight-binding Hamiltonian given in Eq. (1). Our derivation of the tight-binding model is phenomenological in nature and a more microscopic derivation which accounts for the complex environment of the Cu atoms is left for future work.

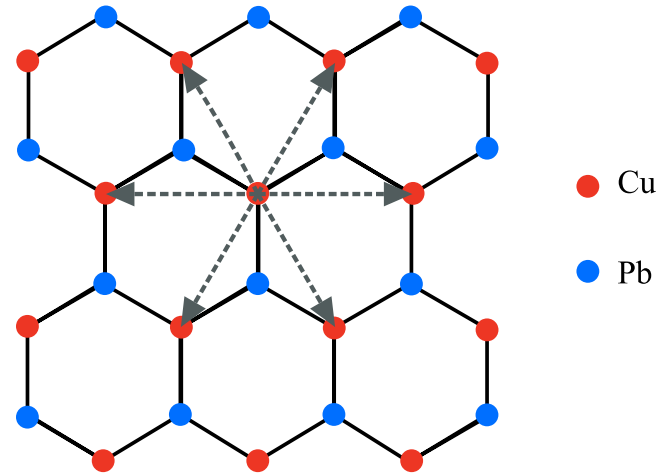

FIG. 1. Pb(1) sites forming a hexagonal lattice in the lead apatite structure. After substitution by copper, one sublattice is occupied by Cu (which we call the A sublattice, in red) and the other one is occupied by Pb (which we call the B sublattice, in blue).

Compared to the two-dimensional four-band model of Ref. [15], we have added k_z dispersion by adding an orbital-independent nearest-neighbor hopping along z. This means the k_z dispersion within our model decouples from the multiorbital physics and simply gives an overall shift of the bands with k_z. This relies on our assumption that we can neglect the small z shift of the $4f$ Wyckoff positions ($z = 0.994$ [17]). Relaxing this assumption would lead to a subleading k_z dependence of the orbital content of the bands, which we do not consider here for simplicity.

The dispersion relation is given by $E_\pm(\mathbf{k}) = d_0(\mathbf{k}) \pm \sqrt{|\mathbf{d}(\mathbf{k})|^2}$ and is shown in Fig. 2. The bottom band is dispersionless along the planar k_x, k_y directions, with energy $E_- = -9/4 - 2t_z\cos(k_z)$. The top band is dispersive, with energy $E_+ = -\frac{1}{4}(3 + 2\sum_{i=1,2,3}\cos(\mathbf{k}\cdot\mathbf{b}_i)) - 2t_z\cos(k_z)$. Our

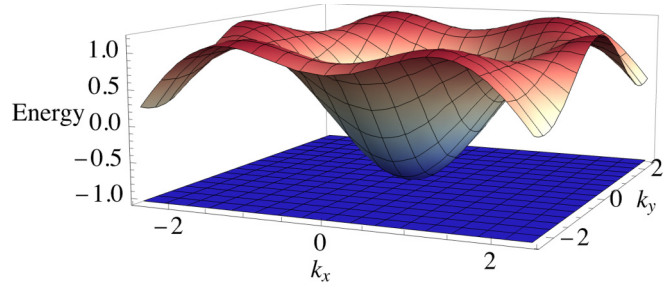

FIG. 2. Surface plot of $E_\pm(\mathbf{k})$ at $k_z = 0$, showing the bottom flat band and the top dispersive band.

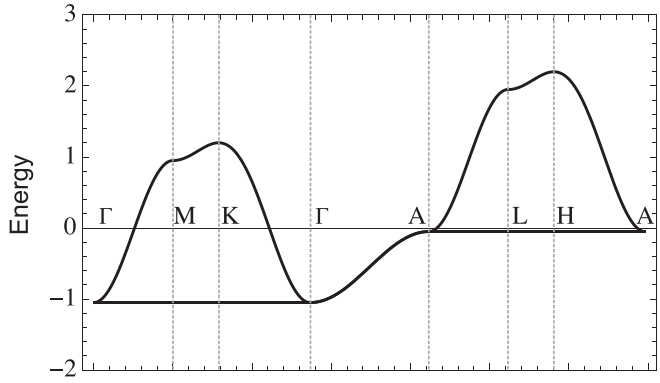

FIG. 3. Dispersion relation $E_{\pm}(\mathbf{k}) - \mu$ with $t_z = 0.25$ and $\mu = -1.7$. Points *A*, *L*, and *H* are all at $k_z = \pi$.

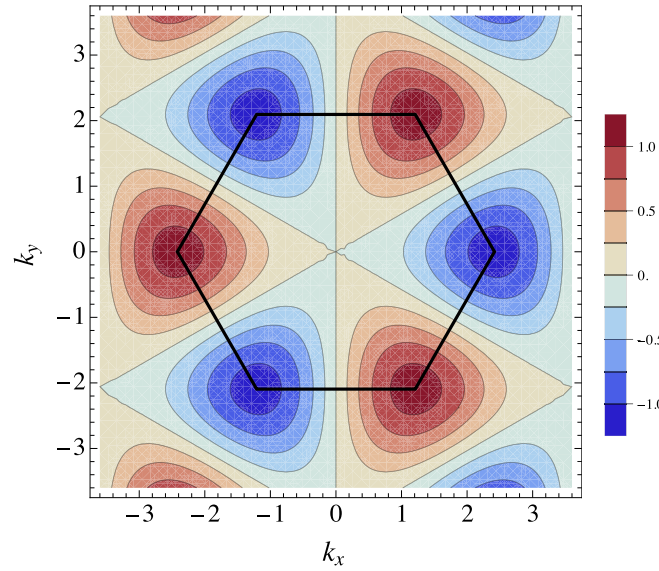

FIG. 4. Contour plot of $\Delta(\mathbf{k}) \propto d_2(\mathbf{k})$ for on-site pairing, showing an f-wave pattern. The Brillouin zone is shown in black.

Hamiltonian is defined in arbitrary units and should be scaled by roughly 0.05 eV to reproduce the bandwidth observed in Ref. [3].

As shown in Fig. 3, our model reproduces the main qualitative features of the two flat bands (see Fig. 4 of Ref. [3]): a top band whose planar dispersion is much larger than the bottom band, a quadratic band touching at the Gamma point, and a simple $\cos(k_z)$-like dispersion for both bands. (In our case, the bottom band is perfectly dispersionless in the plane, but adding further hopping terms would make it possible to change that and reproduce the small dispersion seen in Ref. [3]). We chose a value of the chemical potential $\mu = -1.7$ which reproduces the fact that the top band is roughly half filled at $k_z = 0$. Further, we found that a value of $t_z = 0.25$ reproduces the feature that the bottom band is very close to the Fermi level at $k_z = \pi$.

The fact that the bottom band is perfectly dispersionless in our model arises due to the presence of localized states on the three *A* sites around each hexagon. This is a triangular lattice version of the flat bands arising in the p_x, p_y model on the honeycomb lattice [15]. In fact, for $t_z = 0$, the bands we find have energies which are the square of the bands found in the p_x, p_y honeycomb model [15]. Indeed, the p_x, p_y nearest-neighbor honeycomb model has four bands with dispersion $E_{1,4} = \pm\sqrt{9/4}$ and $E_{2,3} = \pm\sqrt{\frac{1}{4}(3 + 2\sum_{i=1,2,3}\cos(\mathbf{k}\cdot\mathbf{b}_i))}$. This is not surprising, since our tight-binding model can be obtained starting from the four-band model of Ref. [15], as explained above.

We note that our model is not the same as the p_x, p_y model on a triangular lattice considered in Ref. [18]. The reason is that, in our case, the underlying honeycomb lattice breaks inversion symmetry and changes the orbital character of the dominant hopping terms.

It is noteworthy that the dispersive band E_+ has the same dispersion relation as a single-orbital nearest-neighbor model on a triangular lattice (see Fig. 2). However, this simple dispersion relation actually hides a nontrivial k dependence of the orbital character of the bands which is, of course, absent for the single-orbital triangular lattice model. We now discuss the possible implications of this orbital character of the bands for superconductivity and for the orbital magnetic susceptibility.

Superconductivity. Even though the claims of superconductivity in this compound were not confirmed, it is still interesting to study theoretically how the orbital character of the bands in our model constrain the possible superconducting order parameters. Assuming a phonon mechanism for superconductivity, it is natural to consider on-site pairing. We note that the DFT calculations of Ref. [3] predict that the flat bands are perfectly spin-polarized. Assuming that this is indeed the case, the only on-site pairing term allowed by the Pauli principle is an orbital singlet:

$$H_{\mathrm{SC}} = \Delta \sum_{\mathbf{r}} (c^{\dagger}_{\mathbf{r},zx} c^{\dagger}_{\mathbf{r},zy} - c^{\dagger}_{\mathbf{r},zy} c^{\dagger}_{\mathbf{r},zx}) + \mathrm{H.c.} \tag{7}$$

Since, in our model, only the top band crosses the Fermi level, let us keep only intraband pairing terms on the top band [19], leading to

$$H_{\mathrm{SC}} = \sum_{\mathbf{k}} \Delta(\mathbf{k}) c^{\dagger}_{\mathbf{k}} c^{\dagger}_{-\mathbf{k}} + \mathrm{H.c.}, \tag{8}$$

with

$$\Delta(\mathbf{k}) = \Delta(u^*_x(\mathbf{k}) u^*_y(-\mathbf{k}) - u^*_y(\mathbf{k}) u^*_x(-\mathbf{k})), \tag{9}$$

where $(u_x(\mathbf{k}), u_y(\mathbf{k}))$ is the Bloch eigenvector of the top band and where we kept the band index implicit. Using the parametrization $\mathbf{d} = (\sin(\theta)\cos(\phi), \sin(\theta)\sin(\phi), \cos(\theta))$, we have $(u_x, u_y) = (\cos(\theta/2), e^{i\phi}\sin(\theta/2))$. Using the fact that $\theta(\mathbf{k}) = \theta(-\mathbf{k})$ and $\phi(\mathbf{k}) = -\phi(-\mathbf{k})$, one finds $\Delta(\mathbf{k}) \propto d_2(\mathbf{k})$. As seen in Fig. 4, on-site pairing thus generates an f-wave gap of the type $\Delta(\mathbf{k}) \sim k_x(k_x^2 - 3k_y^2)$. We should emphasize that this f-wave gap is on site and is thus microscopically distinct from the non-on-site f-wave gaps which are known to occur in the weak coupling limit of the triangular lattice single-orbital Hubbard model [20]. We also note that interorbital pairing in noncentrosymmetric systems was also discussed in the context of other materials [21], including transition metal dichalocogenides [22].

Assuming an electronic mechanism for superconductivity, one could start from the on-site repulsive interorbital interaction term (which is the only on-site interaction term within our model if we again assume perfectly spin-polarized bands),

$$H_{\text{int}} = U \sum_{\mathbf{r}} n_{\mathbf{r},d_{zx}} n_{\mathbf{r},d_{zy}}, \tag{10}$$

and calculate the effective interaction in the Cooper channel, which would favor non-on-site pairing. Since $U > 0$, and based on the discussion above, on-site repulsion would disfavor any pairing in the f-wave channel. One should thus consider non-on-site pairing in other channels. We note that minimal models featuring d_{zx} and d_{zy} orbitals have been used to study superconductivity in a variety of materials, including pnictides [23] Sr_2RuO_4 [24,25].

Magnetic susceptibility. The magnetic properties of copper-substituted lead apatite were reported to exhibit a combination of soft ferromagnetism and strong diamagnetism [14]. In our model, we have included spin ferromagnetism by fiat by using spin-polarized bands. In addition, the partially filled top band can produce a diamagnetic signal due to orbital effects. Motivated by this possibility, we calculate the out-of-plane orbital magnetic susceptibility of the Hamiltonian of Eq. (1) using the following formula [26–28]:

$$\chi = -\frac{\mu_0 e^2}{2\pi\hbar^2}\text{Im}\int_{-\infty}^{\infty} dE n_F(E) \times \frac{1}{A}\sum_{\mathbf{k}} \text{Tr}\Big[\gamma_x \hat{G}\gamma_y \hat{G}\gamma_x \hat{G}\gamma_y \hat{G} + \frac{1}{2}(\hat{G}\gamma_x\hat{G}\gamma_y + \hat{G}\gamma_y\hat{G}\gamma_x)\hat{G}\frac{\partial\gamma_y}{\partial k_x}\Big], \tag{11}$$

where $\hat{G}(E,\mathbf{k}) = (E - H_{\mathbf{k}} + i\eta)^{-1}$, $\gamma_{x,y} = \frac{\partial \hat{H}_{\mathbf{k}}}{\partial k_{x,y}}$, μ_0 is the vacuum permeability, η is a small positive number, A is the sample area, and $n_F(E) = (e^{(E-\mu)/T} + 1)^{-1}$ is the Fermi distribution function. For the rest of the discussion, we will work at $T = 0$. The results for the susceptibility are shown in Fig. 5. Since in our 3D model [Eq. (1)], the k_z dependence simply corresponds to an overall shift of the bands with k_z, one can absorb the k_z dependence into a k_z-dependent chemical potential $\mu(k_z)$. This means we only need to do a two-dimensional calculation for the orbital susceptibility [i.e., with $t_z = 0$ in Eq. (1)]. The value of the orbital susceptibility for a given k_z slice can be read from Fig. 5 by looking at the value of the chemical potential which is relevant for that k_z value, following $\mu(k_z) = \mu_0 + 2t_z\cos(k_z)$, where μ_0 is the actual value of the chemical potential in the 3D model.

One notable advantage of employing Eq. (11) over the Peierls-Landau orbital susceptibility method [29–31] is that it accounts for contributions originating from the quantum geometry of the Bloch wave functions, which has been shown to play a crucial role in multiorbital models [32–34].

In this context, it is instructive to compare the susceptibility of our model with that of a single-orbital, nearest-neighbor triangular lattice Hamiltonian, with dispersion $E_{s.o} = -\frac{3}{4} - \frac{1}{2}\sum_{i=1}^{3}\cos(\mathbf{k}\cdot\mathbf{b}_i)$. As noted before, this single-band Hamiltonian has exactly the same dispersion as the upper band of our two-band model. By comparing these two models, we can thus elucidate the specific impact of multiorbital physics on the orbital susceptibility.

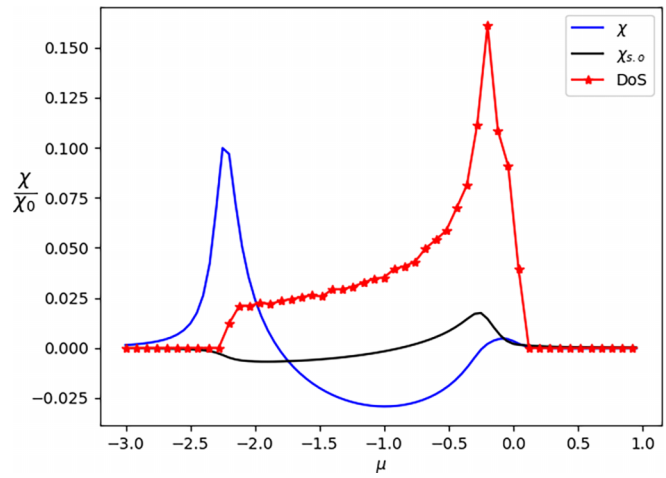

FIG. 5. Orbital susceptibility for our two-band model χ (in blue) and for a single-orbital model $\chi_{s.o}$ (in black). The density of states (DOS) of the top band E_+ (which is the same as the the DOS of the single-orbital model) is also shown in red. We have $\chi_0 = \frac{\mu_0 e^2 |t| a^2}{\hbar^2}$, with $|t|$ the magnitude of the nearest-neighbor hopping term, and a the lattice spacing between copper sites. The DOS is in units of $\frac{1}{|t|a^2}$. We used $\eta = 0.1$ to calculate the susceptibilities.

The results for the single-orbital model are easily interpreted: At low filling, there is a single pocket around the gamma point and lattice effects become negligible, leading to a negative value for $\chi_{s.o}$, as it should to recover Landau diamagnetism of free electrons. At larger filling, the system goes through a van Hove singularity, at which the Fermi surface changes topology and at which the DOS diverges. This van Hove singularity produces a paramagnetic peak for $\chi_{s.o.}$, which is a well-known effect [31].

Interestingly, the susceptibility of our two-band model χ has very different features. First, there is a paramagnetic peak at low filling (for $-2.5 < \mu < -2$), which is due to the presence of the bottom flat band E_-. Second, there is a broad region of diamagnetism for $-1.75 < \mu < -0.25$, despite the presence of a van Hove singularity close to $\mu = -0.25$. We note that the single-orbital model is paramagnetic in the range $-1.75 < \mu < -0.25$ due to the van Hove singularity, and the diamagnetism of the two-orbital model thus has a multiorbital origin. The diamagnetism in this region is comparatively strong: the most negative value reached by χ for $\mu \simeq -1$ is about four times larger than the one reached by $\chi_{s.o}$ at low filling. The strong diamagnetism we observe in the two-band model could thus provide an explanation for the one reported in experiments [14]. However, diamagnetism could also be explained by the presence of unintended Cu_2S in the samples [14,35] (which is a known diamagnet [36]).

In conclusion, we have proposed a minimal two-band model which reproduces the main features of the Cu d_{zx} and d_{zy} flat bands predicted to appear in a copper-substituted lead apatite in Ref. [3]. Using this model, we have found a strong diamagnetic response which could explain the one observed in experiments, and whose origin lies in the multiorbital nature of the bands.

In this paper, we focused on reproducing the main features of the band structure predicted by Ref. [3] for $CuPb_9(PO_4)_6(OH)_2$. However, we should mention several caveats regarding the applicability of these predictions to real samples of LK-99. First, samples could alternatively contain O instead of $(OH)_2$ anions due to the existence of the the closely related $CuPb_9(PO_4)_6O$ structure. Second, substitution sites for copper could also alternate between different Pb(1) sites, and even Pb(2) sites, leading to disorder. Studying the impact of such disorder on flat-band physics would require further work. Nevertheless, looking beyond its applicability to LK-99, our two-orbital model provides an interesting toy model to study strongly correlated and multiorbital physics.

Note added. Recently, other tight-binding models capturing the flat bands of copper-substituted lead apatite were proposed [17,37–40].

Acknowledgments. T.S. gratefully acknowledges discussions with S. White, J. Sanchez-Yamagishi, and F. Gonzalez.

[1] S. Lee, J.-H. Kim, and Y.-W. Kwon, The first room-temperature ambient-pressure superconductor, arXiv:2307.12008.

[2] S. Lee, J. Kim, H.-T. Kim, S. Im, S. An, and K. H. Auh, Superconductor $Pb_{10-x}Cu_x(PO_4)_6O$ showing levitation at room temperature and atmospheric pressure and mechanism, arXiv:2307.12037.

[3] S. M. Griffin, Origin of correlated isolated flat bands in copper-substituted lead phosphate apatite, arXiv:2307.16892.

[4] J. Lai, J. Li, P. Liu, Y. Sun, and X.-Q. Chen, First-principles study on the electronic structure of $Pb_{10-x}Cu_x(PO_4)_6O$ ($x = 0, 1$), J. Mater. Sci. Technol. **171**, 66 (2023).

[5] L. Si and K. Held, Electronic structure of the putative room-temperature superconductor $Pb_9Cu(PO_4)_6O$, Phys. Rev. B **108**, L121110 (2023).

[6] R. Kurleto, S. Lany, D. Pashov, S. Acharya, M. van Schilfgaarde, and D. S. Dessau, Pb-apatite framework as a generator of novel flat-band CuO based physics, including possible room temperature superconductivity, arXiv:2307.16892.

[7] J. Cabezas-Escares, N. F. Barrera, C. Cardenas, and F. Munoz, Theoretical insight on the LK-99 material, arXiv:2308.01135.

[8] D. Pashov, S. Acharya, S. Lany, D. S. Dessau, and M. van Schilfgaarde, Multiple Slater determinants and strong spin-fluctuations as key ingredients of the electronic structure of electron- and hole-doped $Pb_{10-x}Cu_x(PO4)_6O$, arXiv:2308.09900.

[9] L. Celiberti, L. Varrassi, and C. Franchini, $Pb_9Cu(PO_4)_6O$ is a charge-transfer semiconductor, Phys. Rev. B **108**, L201117 (2023).

[10] T. T. Heikkilä, N. B. Kopnin, and G. E. Volovik, Flat bands in topological media, JETP Lett. **94**, 233 (2011).

[11] N. B. Kopnin, T. T. Heikkilä, and G. E. Volovik, High-temperature surface superconductivity in topological flat-band systems, Phys. Rev. B **83**, 220503(R) (2011).

[12] J. S. Hofmann, E. Berg, and D. Chowdhury, Superconductivity, pseudogap, and phase separation in topological flat bands, Phys. Rev. B **102**, 201112(R) (2020).

[13] P. Törmä, S. Peotta, and B. A. Bernevig, Superconductivity, superfluidity and quantum geometry in twisted multilayer systems, Nat. Rev. Phys. **4**, 528 (2022).

[14] P. Wang, X. Liu, J. Ge, C. Ji, H. Ji, Y. Liu, Y. Ai, G. Ma, S. Qi, and J. Wang, Ferromagnetic and insulating behavior in both half magnetic levitation and non-levitation LK-99 like samples, Quantum Front **2**, 10 (2023).

[15] C. Wu, D. Bergman, L. Balents, and S. Das Sarma, Flat bands and Wigner crystallization in the honeycomb optical lattice, Phys. Rev. Lett. **99**, 070401 (2007).

[16] X. Hao, W. Wu, J. Zhu, B. Song, Q. Meng, M. Wu, C. Hua, S. A. Yang, and M. Zhou, Topological band transition between hexagonal and triangular lattices with (p_x, p_y) orbitals, J. Phys.: Condens. Matter **34**, 255504 (2022).

[17] Y. Jiang, S. B. Lee, J. Herzog-Arbeitman, J. Yu, X. Feng, H. Hu, D. Călugăru, P. S. Brodale, E. L. Gormley, M. Garcia Vergniory, C. Felser, S. Blanco-Canosa, C. H. Hendon, L. M. Schoop, and B. A. Bernevig, $Pb_9Cu(PO4)_6(OH)_2$: Phonon bands, localized flat band magnetism, models, and chemical analysis, arXiv:2308.05143.

[18] H.-H. Hung, W.-C. Lee, and C. Wu, Frustrated cooper pairing and f-wave supersolidity in cold-atom optical lattices, Phys. Rev. B **83**, 144506 (2011).

[19] As long as the temperature is substantially smaller than the bandwidth (which is estimated from DFT to be 0.1 eV, which corresponds roughly to 1000 K), it should be safe to neglect pairing on the bottom band which does not cross the Fermi level.

[20] S. Raghu, S. A. Kivelson, and D. J. Scalapino, Superconductivity in the repulsive Hubbard model: An asymptotically exact weak-coupling solution, Phys. Rev. B **81**, 224505 (2010).

[21] Y. Fukaya, S. Tamura, K. Yada, Y. Tanaka, P. Gentile, and M. Cuoco, Interorbital topological superconductivity in spin-orbit coupled superconductors with inversion symmetry breaking, Phys. Rev. B **97**, 174522 (2018).

[22] G. Margalit, E. Berg, and Y. Oreg, Theory of multi-orbital topological superconductivity in transition metal dichalcogenides, Ann. Phys. **435**, 168561 (2021).

[23] S. Raghu, X.-L. Qi, C.-X. Liu, D. J. Scalapino, and S.-C. Zhang, Minimal two-band model of the superconducting iron oxypnictides, Phys. Rev. B **77**, 220503(R) (2008).

[24] S. Raghu, A. Kapitulnik, and S. A. Kivelson, Hidden quasi-one-dimensional superconductivity in S_2RuO_4, Phys. Rev. Lett. **105**, 136401 (2010).

[25] T. Scaffidi, Degeneracy between even- and odd-parity superconductivity in the quasi-one-dimensional Hubbard model and implications for S_2RuO_4, Phys. Rev. B **107**, 014505 (2023).

[26] M. Koshino and T. Ando, Orbital diamagnetism in multilayer graphenes: Systematic study with the effective mass approximation, Phys. Rev. B **76**, 085425 (2007).

[27] G. Gómez-Santos and T. Stauber, Measurable lattice effects on the charge and magnetic response in graphene, Phys. Rev. Lett. **106**, 045504 (2011).

[28] A. Gutiérrez-Rubio, T. Stauber, G. Gómez-Santos, R. Asgari, and F. Guinea, Orbital magnetic susceptibility of graphene and MoS_2, Phys. Rev. B **93**, 085133 (2016).

[29] H. Fukuyama, Theory of orbital magnetism of Bloch electrons: Coulomb interactions, Prog. Theor. Phys. **45**, 704 (1971).

[30] S. A. Safran and F. J. DiSalvo, Theory of magnetic susceptibility of graphite intercalation compounds, Phys. Rev. B **20**, 4889 (1979).

[31] G. Vignale, Orbital paramagnetism of electrons in a two-dimensional lattice, Phys. Rev. Lett. **67**, 358 (1991).

[32] A. Raoux, M. Morigi, J.-N. Fuchs, F. Piéchon, and G. Montambaux, From dia- to paramagnetic orbital susceptibility of massless fermions, Phys. Rev. Lett. **112**, 026402 (2014).

[33] F. Piéchon, A. Raoux, J.-N. Fuchs, and G. Montambaux, Geometric orbital susceptibility: Quantum metric without berry curvature, Phys. Rev. B **94**, 134423 (2016).

[34] A. Raoux, F. Piéchon, J.-N. Fuchs, and G. Montambaux, Orbital magnetism in coupled-bands models, Phys. Rev. B **91**, 085120 (2015).

[35] P. K. Jain, Superionic phase transition of copper(I) sulfide and its implication for purported superconductivity of LK-99, J. Phys. Chem. C **127**, 18253 (2023).

[36] C. I. Pearce, R. A. Pattrick, and D. J. Vaughan, Electrical and magnetic properties of sulfides, Rev. Mineral. Geochem. **61**, 127 (2006).

[37] M. M. Hirschmann and J. Mitscherling, Minimal model for double Weyl points, multiband quantum geometry, and singular flat band inspired by LK-99 (2023), arXiv:2308.03751.

[38] P. A. Lee and Z. Dai, Effective model for $Pb_9Cu(PO_4)_6O$, arXiv:2308.04480.

[39] C. Yue, V. Christiansson, and P. Werner, Correlated electronic structure of $Pb_{10-x}Cu_x(PO4)_6O$, Phys. Rev. B **108**, L201122 (2023).

[40] N. Mao, N. Peshcherenko, and Y. Zhang, Wannier functions, minimal model and charge transfer in $Pb_9CuP_6O_{25}$, arXiv:2308.05528.